Lubricated sliding wear mechanism of chromium-doped graphite-like carbon coating

MANDAL, Paranjayee, EHIASARIAN, Arutiun <http://orcid.org/0000-0001-6080-3946> and HOVSEPIAN, Papken <http://orcid.org/0000-0002-1047-0407>

Published version

MANDAL, Paranjayee, EHIASARIAN, Arutiun and HOVSEPIAN, Papken (2014). Lubricated sliding wear mechanism of chromium-doped graphite-like carbon coating. Tribology International, 77, 186-195.

Lubricated sliding wear mechanism of Chromium doped graphite-like carbon coating

Paranjayee Mandal*[1], Arutiun P. Ehiasarian[2] and Papken Eh. Hovsepian[3]

Nanotechnology Centre for PVD Research, HIPIMS Research Centre, Sheffield Hallam University, City Campus, Howard Street, Sheffield S1 1WB, United Kingdom

Email: 200712mum@gmail.com*[1], a.ehiasarian@shu.ac.uk[2] , p.hovsepian@shu.ac.uk[3]

Abstract

The current research aims to discuss the tribological behaviour of Chromium-doped graphite-like carbon coatings and suggest a wear mechanism under both dry (in air) and boundary lubricated sliding condition based on phase composition of the wear product generated in wear track during pin-on-disc experiments. As expected, the friction coefficient reduces from 0.22 to 0.12 due to addition of lubricant. Raman analysis indicates that wear mechanism is oxidative in dry sliding condition whereas it is chemically reactive in the presence of lubricant. It is speculated that the key-factor of reduced friction and wear coefficient in lubricated condition is the formation of $CrCl_3$ due to tribochemical reaction between coating and oil. $CrCl_3$ has graphite-like layered structure; therefore it acts like solid lubricant.

Keywords: C/Cr, Dry and lubricated sliding, Raman spectroscopy, Wear mechanism

1. Introduction

Low friction is one of the various aspects that help to improve the engine performance. Reduced friction in moving engine components can be achieved either by using better-quality lubricants (engine oils) or by coating the automotive engine components using suitable tribological coatings. These coatings should have low friction, improved wear resistance and high thermal stability as they have to withstand high mechanical loads and high wear when operating in hostile environment. The performance of these coatings is further enhanced (achieving lower friction (μ) and wear coefficient (K_c)) in the presence of the lubricant. The lubricant or the engine oil usually contains different polymer additives and friction modifiers promoting low friction due to the formation of a thin tribolayer on the sliding surfaces. With reduction in friction coefficient, the energy consumption becomes lower and fuel economy is improved. However, such oils are costly and products of the chemical reaction between the oil and the sliding surfaces can contaminate the oil leading to shorter lifetime. This problem can be eliminated if the coating of the sliding surfaces is inactive to engine oil or if the coating itself produces some lubricious compounds that do not pollute the oil by tribochemical reactions during sliding.

Amorphous carbon coatings are very commonly used as tribobological coatings due to their excellent friction and wear properties (μ <0.1 and K_c <10^{-17} $m^3N^{-1}m^{-1}$) [1], high hardness (>20 GPa) [1, 2] and chemical inertness. Depending on the ratio of sp^2 (graphite-like) to sp^3 (diamond-like) bonded carbons, the amorphous carbon coatings can adapt either graphite-like or diamond-like properties or a combination of properties within this range [3, 4]. Graphitic carbon coatings have lower friction and wear coefficients (μ <0.1 and K_c ~10^{-17} $m^3N^{-1}m^{-1}$ respectively) when compared to diamond-like-carbon (DLC) coatings (μ ~0.15 and K_c ~10^{-16} $m^3N^{-1}m^{-1}$ respectively) in dry atmosphere environment [2]. DLC coatings provide excellent friction properties (μ =

0.007 – 0.4) in vacuum (below 10^{-4} Pa) [2, 4, 5] along with varying hardness values (10 – 80 GPa) [2, 4, 6] depending on the deposition process. Nevertheless, the use of DLC coatings is restricted due to high compressive residual stress (up to 13 GPa) [4], poor coating adhesion and poor thermal stability with graphitisation starting at ~350˚C [7]. One way to ensure strong adhesion between DLC coating and the substrate is to deposit an in-situ carbon interlayer before the deposition. This can be achieved by pulsed laser deposition (PLD) process in which very low pulses (of the order of femto-seconds) are used along with a high power density (up to 10^{-13} W/cm^2). The process provides high kinetic energy (up to 1 keV) to the impinging carbon atoms, which finally embed into the substrate. The firm embedding of the carbon atoms increases the adhesion strength of the DLC coating with the substrate [3]. In addition to this, a small quantity of transitional metal dopants such as W, Mo, Cr, Si into the DLC films can improve the coating adhesion (hence, relaxation of internal residual stresses) along with its hardness, modulus, thermal and friction properties. That is, doping with Si, Ti, Cr or W results in lower internal residual stress [3, 7 − 12] and higher thermal stability [7, 8], whereas low friction coefficient is achieved when Cr, Si and Mo are used as dopants [8 − 10, 13]. Both the DLC and metal-doped DLC films can be deposited using PVDs (ion beam assisted, cathodic arc, RF sputtering, magnetron sputtering), CVD and laser ablation processes (laser cladding, pulsed laser deposition) [3].

Chromium containing Carbon coatings have an excellent combination of higher thermal stability (oxidation starts ~400˚C) [14], reduced internal compressive residual stress (0.7 – 1.14 GPa) [15, 16], lower friction coefficient (0.08 – 0.16) [2, 16] and wear coefficient (10^{-16} – 10^{-18} m^{3}N^{-1}m^{-1}) [2, 11, 15, 16] and reasonable hardness (12 – 40 GPa) [2, 15, 16]. Therefore, they can be considered as one of the potential candidates that meet the

requirements of improved tribological properties (lower friction and wear coefficients) along with higher thermal stability for operating in hostile environment.

The wear and friction behaviour of this coating has already been extensively studied [2, 10, 16 − 23] however, only a few reports have been found explaining the wear mechanism during dry sliding [10, 16, 18, 19] and no publications have been found reporting on their tribological behaviour as well as wear mechanism in lubricated sliding condition. Moreover, the tribological properties are found to be very much dependent on the coating deposition technique, amount of Cr content present in the film and various test parameters adopted during sliding. The influence of these factors in controlling the friction and wear coefficients and wear mechanism during sliding in dry and lubricated condition has been discussed in detail in the following section.

1.1. Tribological behaviour of state-of-the-art Chromium doped Carbon coatings

Among Cr-doped carbon coatings, the friction coefficient reported in the literature ranges from 0.06 to 0.4 depending on the tribopairs used during dry sliding in open-air condition [16 − 19, 22]. In lubricated sliding of Cr-doped diamond like carbon (Cr-DLC) films, the friction coefficient has been reduced to the range of 0.05 – 0.15 depending on the various combinations of lubricant used [20].

On the other hand, Cr doped graphitic carbon coatings (C/Cr) show a wide range of friction coefficient during dry sliding in air depending on the selection of the test parameters. The friction coefficient of C/Cr coating has been found in the range of 0.06 – 0.23 in air [2, 10, 21] but it becomes significantly higher (0.7 – 0.8) when tested in dry

nitrogen environment [21]. In water-lubricated condition, the friction coefficient of C/Cr coatings reduces to 0.1 – 0.33 [23]. The wear coefficient of Cr-based carbon coatings has been reported ~10^{-16} − 10^{-18} $m^3N^{-1}m^{-1}$ [2, 10, 16 − 19, 22] during dry sliding in air condition. In lubricated condition, the wear coefficient has been reported the range of ~10^{-15} – 10^{-16} $m^3N^{-1}m^{-1}$) [20, 23].

1.1.1. Tribological behaviour in dry sliding condition

The Cr-DLC film deposited using a hybrid sputtering ion beam system (DC magnetron sputtering and linear ion source), has shown friction coefficient >0.2 against steel ball (HRC60) for 500 m sliding distance and 1 N applied load [17]. The wear coefficient (~3 × 10^{-17} $m^3N^{-1}m^{-1}$) has been found slightly higher compared to pure DLC film (~2.6 × 10^{-17} $m^3N^{-1}m^{-1}$) [17]. The friction coefficient of the Cr-DLC film deposited using hybrid PVD and PECVD process, has been reported <0.2 against 440C SS and alumina (Al_2O_3) balls for 1000 m sliding distance and 2.5 N applied load [18]. It has been found that Cr-DLC coating with <4.8 at.% Cr has friction and wear coefficient (μ <0.14 and K_c ~10^{-16} $m^3N^{-1}m^{-1}$ respectively) higher than pure DLC film. This behaviour has been explained by the presence of hard Chromium carbide particles, which act as a third-body in the tribocontact causing interruption in the tribolayer formed during sliding [18]. This fact is supported by another study, where different Cr-DLC films are deposited using a hybrid ion beam (DC magnetron sputtering and linear ion source) deposition system [19]. In this case, the friction coefficients have been reported to increase from 0.15 to 0.3 depending on Cr content present in the film when sliding against steel ball (HRC60) for 300 m sliding distance and 3 N applied load. A drastic rise in wear rate (~8.9 × 10^{-18} $m^3N^{-1}m^{-1}$ to ~1.4 × 10^{-16} $m^3N^{-1}m^{-1}$) with increasing Cr content in the film has been attributed to the abrasive wear caused by the hard Chromium carbide particles during sliding [19]. One more study

has established a similar fact by explaining the tribological behaviour of pure DLC and Cr-DLC coatings against 440C SS ball during 1000 m of dry sliding in open air [16]. In this study, both the coatings have been deposited using reactive magnetron sputtering in an intensified plasma-assisted coating system. The friction and wear coefficients of pure DLC coating ($\mu \sim 0.09$ and $K_c \sim 0.93 \times 10^{-16}$ $m^3N^{-1}m^{-1}$ respectively) have been reported lower when compared to the Cr-DLC coating ($\mu \sim 0.11$ and $K_c \sim 1.37 \times 10^{-16}$ $m^3N^{-1}m^{-1}$ respectively). The presence of Cr-rich nanoparticles is believed to interrupt the transfer layer formation during sliding, therefore is found to be responsible for achieving higher friction and wear coefficient [16].

The tribological behaviour of Cr-DLC coatings deposited using a hybrid technique (vacuum arc evaporation and magnetron sputtering for Cr/C intermediate layers and RF PACVD for depositing outer DLC layer) has been found very much dependent on the tribopairs used in the dry sliding conditions [22]. Three different counterparts, alumina (Al_2O_3), uncoated 100Cr6 and Cr-DLC coated 100Cr6 balls, have been tested during sliding in open-air condition under two different parametric settings ((a) 10 km sliding distance for 20 N normal loads and (b) 1 km sliding distance for 80 N normal loads). Irrespective of the parametric settings, the highest friction coefficients (in the range of 0.15 ─ 0.4 for setting (a) and 0.1 ─ 0.3 for setting (b)) have been reported for Cr-DLC/uncoated 100Cr6 tribopair compared to others. For parameter set (a), steady state friction coefficients of ~0.12 and ~0.1 have been reported for Cr-DLC/Cr-DLC coated 100Cr6 and Cr-DLC/ Al_2O_3 tribopairs respectively after 2000 m of sliding. On the other hand, friction coefficients have been reduced to ~0.06 and ~0.08 for Cr-DLC/Cr-DLC coated 100Cr6 and Cr-DLC/ Al_2O_3 tribopairs respectively under parameter set (b). The measurement of wear rates indicate that the wear rate of coating ($K_{vc} = 3.2 - 3.8 \times 10^{-17}$

$m^3N^{-1}m^{-1}$) is almost similar for all the counterparts; however their wear rate decreases with increasing hardness [22].

The tribological properties of C/Cr film deposited using DC unbalanced magnetron sputtering have been reported against WC-6%Co ball for 720 m sliding distance and varying normal load of 10 – 80 N. The friction and wear coefficients have been found in the range of 0.08 – 0.16 and 10^{-18} – 10^{-16} $m^3N^{-1}m^{-1}$ respectively and both of them varies depending on the coating hardness [2]. The same C/Cr coating has been tested further with a different parametric setting of varying normal load (20 – 80 N) and sliding distance (400 – 1000 m) under dry condition. The friction coefficient decreases linearly 0.09 – 0.06 with increasing applied load 20 – 80 N, however, the wear coefficient (K_c ~10^{-17} $m^3N^{-1}m^{-1}$) is found almost unaffected. The wear mechanism in dry sliding has been explained in detail in this paper. The combined effect of presence of moisture in the test environment and the third-body abrasion during sliding has been held responsible for achieving low wear coefficient whereas the reorientation of graphite nanocrystallised clusters to preferable (002) planes has been attributed to attain low friction coefficient during sliding [10].

The influence of moisture on the friction behaviour of C/Cr film has been supported in another study, in which C/Cr film has been deposited using combined steered cathodic arc and unbalanced magnetron sputtering [21]. The dry sliding test has been conducted in open air (~30% humidity) and dry nitrogen (almost ~0% humidity) environment against 100Cr6 ball for 500 m sliding distance and 5 N applied load. The friction coefficient has been found much lower (0.21 ─ 0.23) for open air when compared to dry nitrogen environment (0.7 ─ 0.8). It is believed that water particles in the test environment reduce the adhesive interactions between sliding surfaces by forming a transfer layer during sliding, which helps in reducing friction coefficient in open air. However, in dry nitrogen

environment, formation of such transfer layer is not possible; therefore high friction and rapid wear is observed [21].

1.1.2. Tribological behaviour in lubricated sliding condition

The tribological behaviour of Cr-DLC coatings in lubricated sliding has been reported in detail [20]. Cr-DLC coatings with varying Cr content (0% − 23.3%) have been deposited using hybrid technique (a combination of magnetron sputtering, vacuum cathodic arc sources and linear anodic layer ion sources) by controlling the Cr target current. The Si_3N_4 ball has been used as counterpart during sliding tests for a sliding distance of 2300 m and applied load of 9.8 N under different lubrication conditions. Polyalphaolefin synthetic oil (PAO-4) and paraffin-based mineral oil (150SN) have been chosen as base lubricants and molybdenum dithiocarbamate (Mo-DTC) and amine sulphuric-phosphate diester (T307) have been selected as a friction modifier and an extreme pressure (EP) additive respectively. The influences of base oil and base oil with friction modifier and EP additive have been investigated in detail. It has been found that the Cr content present in the DLC films has no significant effect in reduction of friction coefficient (courtesy: ref [20], figure 4a, 4b, 4e and 4f) during sliding tests performed in base oils and base oils with T307 combinations. However with the addition of Mo-DTC in the base oils, the friction coefficient has been influenced by the Cr content present in the coating (courtesy: ref [20], figure 4c and 4d). In this case, the lowest friction coefficient has been reported for Cr-DLC with 0.2% Cr content compared to other Cr-doped DLC coatings. The wear coefficient of the same coating (Cr-DLC with 0.2% Cr content) has been found low ($<1 \times 10^{-16}$ $m^3N^{-1}m^{-1}$) irrespective of all lubricant combinations and this behaviour has been attributed to the high hardness of this coating (>15 GPa). However, wear coefficients of other Cr-doped coatings have been reported in the range of $1 \times 10^{-16} - 7 \times 10^{-16}$ $m^3N^{-1}m^{-1}$ (courtesy: ref [20], figure 5a and 5b). This paper concludes that the doping of Cr at an

optimal level (0.2%) increases the wear resistance. Yet, it does not provide any information about the wear mechanism during lubricated sliding.

Another study shows the tribological performance of a C/Cr multilayer coating deposited by magnetron sputtering in water-lubricated environment [23]. The friction coefficient has been found 0.1 ─ 0.33 against polished Al_2O_3 ball for 273 m of sliding distance and 5 N of applied load. The high wear rate of this coating generates debris, which has been found to adhere to the pin surface forming a thick layer. The wear coefficient has been found to be less than 0.01×10^{-15} $m^3N^{-1}m^{-1}$ [23]. No information on wear mechanism during sliding has been discussed in this paper.

Summarising the above facts, it can be understood that the tribological behaviour of Cr-based carbon coatings is well established and the wear mechanism in dry sliding has already been explained by several researchers. The tribological behaviour in lubricated sliding of this class of coatings has also been documented however, no information has been reported clarifying the wear mechanism. Hence, this paper aims to discuss the tribological behaviour based on the phase composition of the wear product generated in the wear track during pin-on-disc experiments and the paper suggests a wear mechanism of the C/Cr coating under both dry and boundary lubricated sliding condition (using commercially available synthetic engine oil as lubricant).

2. Experimental details

2.1. Coating deposition process

C/Cr coatings have been deposited on hardened (62 HRC) high speed steel substrate by a combined steered cathodic arc and unbalanced magnetron process known as Arc-Bond-

Sputtering (ABS) [24], using an industrial sized HTC 1000-4 PVD coater by Hauzer Techno Coating. The deposition system is equipped with four cathodes furnished with three graphite targets and a Chromium target as shown in Figure 1. The coating is produced in three separate steps: (i) Cr^+ metal ion etching, (ii) CrN base layer deposition, (iii) C/Cr nanostructured multilayer (with a bilayer thickness of <2 nm) [25] coating deposition. During the first step of the process, single and multiple charged Cr metal ions produced by arc evaporation were accelerated towards the substrate using high bias voltage of -1200 V to sputter clean the surface and implant Cr in order to enhance coating adhesion. For further enhancement of the adhesion, a base layer of CrN was deposited by sputtering of Cr in a mixed nitrogen-argon atmosphere at a substrate bias of -75 V. Then the C/Cr coating was deposited for 4 hours by simultaneous sputtering of Cr and C in nonreactive argon atmosphere. More details of the experimental procedure have been discussed elsewhere [21].

2.2. Characterisation techniques

2.2.1. Pin-on-disc test

A CSM room temperature pin-on-disc tribometer has been used to study the friction behaviour of the deposited coatings in both dry and lubricated sliding condition. The tribometer comprises a stationary ball as counterpart, which slides against the coated disc sample clamped to a rotating sample holder under the influence of a static load. The system calibration procedure includes the friction force and motor speed. A load cell of 5 N is used to measure and calibrate the friction force. Uncoated 100Cr6 steel balls of 6 mm diameter are used as counterpart. The static load and the sliding distance are fixed to 5 N and 5 km respectively for the current experiments. The room temperature and the relative humidity recorded for the experiments are 25°C and 15% respectively. The coefficient of friction is calculated as $\mu = F_T/F_N$, where F_T is tangential force and F_N is normal force.

The highly viscous Mobil1 Extended life^{TM} 10W-60 multigrade synthetic engine oil is used as lubricant in lubricated sliding. This oil contains different polymer additives to achieve low friction however, it is free of friction modifiers. Sulphated ash (1.4 wt%) and phosphorus compounds (0.13 wt%) are the main ingredients of this oil [26]. Sulphated ash is composed of sulphur and chlorine compounds and different metal additives including K, Ba, Ca, Mg, Na and sometimes Sn and Zn. The metal additives are more reactive to phosphorus compounds compared to sulphur and chlorine compounds. Therefore, if the oil contains phosphorus compounds, the metal additives react with them under suitable conditions and produce metal phosphates and metal oxides (applicable for Sn and Zn only). The resulting sulphur and chlorine compounds become free to react chemically with other metals if present in the system under appropriate temperature and other operating conditions [27].

The wear coefficient was calculated using Archard's equation as $K_C = \frac{V}{F_N * d}$ where V is wear volume in m^3, F_N is normal load in N and d is the sliding distance in meter. The wear volume V is calculated as $V = 2\pi RA$, where R is wear track radius and the A is cross sectional area of the wear track measured by Veeco Dektak surface profilometer.

2.2.2. Raman spectroscopy

The Raman spectra were collected from random positions on the wear track after individual sliding in different test conditions (dry and lubricated) using a Horiba-Jobin-Yvon LabRam HR800 integrated Raman spectrometer fitted with green laser (wavelength 532 nm). A 10 % transmission filter was used to reduce the intensity of incident beam and to avoid irradiation damage. The wear tracks were exposed to green laser after both dry and lubricated sliding for 120 s for spectrum collection. The Raman spectrum was

averaged over 5 acquisitions in the wavelength range of 50 – 2250 cm^{-1} for each test condition. During analysis, the background of spectra was corrected using a 2^{nd} order polynomial whereas a multi-peak (8–10) Gaussian-fitting function was used to deconvolute the spectrum and identify the Raman peaks. A two-peak Gaussian-fitting function was seldom capable of analysing the spectrum obtained for a random distribution of phonon lifetimes in a disordered material. An alternative to the Gaussian-fitting was a Breit-Wigner-Fano (BWF) line for G peak and a Lorenzian (L) line for D peak fitting [28]. However, two-peak Gaussian-fitting function was used by researchers in analysing the Raman spectra [29 – 33]. Later, it was established that the multi-peak (at least 4 peaks) Gaussian-fitting function was similar to that of combined BWF (for G peak) and L (for D peak) fitting and both the methods gave similar I_D/I_G ratio [34]. Based on the applicability of the deconvoluting techniques, the multi-peak Gaussian-fitting function was chosen for the current study. The same parameter settings were used to accumulate the spectrum from pure Cr_2S_3 powder. The powder was analysed as no data on Raman scattering from this compound was available to us. The spectrum from thin engine oil film placed on a glass slide was collected using the same acquisition settings but the collection time and the wavelength range was set different. The oil film was exposed to green laser for 10s in order to avoid the chance of burning the oil. The Raman spectrum was acquired for 5 times in the wavelength range of 100 – 2200 cm^{-1} and their average was plotted. The background of the spectrum was corrected using straight line during analyses. However, peaks could not be identified because the exact chemical compounds present in the oil are unknown.

3. Results

3.1. Tribological properties

Figure 2 shows the friction behaviour of C/Cr coating under both dry and lubricated sliding condition. It can be seen that the average value of the coefficient of friction after 5 km of dry sliding has been reduced by ~45.5% from 0.22 to 0.12 due to adding a lubricant. It is well known that in every tribological pair during sliding wear particles will be generated. The wear debris trapped in between sliding surfaces where they undergo severe deformation and chemical reactions with the environment, which determines the friction coefficient value. Apart from the third-body interaction between the wear particles and the sliding surfaces of the tribological contact the coefficient of friction is strongly influenced by the humidity in the test environment. It has been reported that the water molecules present in the test environment react with the carbon based film and form a very thin layer [3]. However, during sliding, this layer is periodically removed and reformed due to the wear process taking place in the tribo-contact [3]. This ultimately results in stick-slip motion, which produces variation in the friction value. On the other hand, the friction curve in lubricated sliding is very smooth and no stick-slip motion is noticeable. Moreover, the initial run-in period in lubricated sliding is very short unlike that of dry sliding.

Figure 3 shows the wear track profiles after dry and lubricated sliding as measured by surface profilometer. For sliding in air after 5 km, the wear track was found to be ~1.2 μm deep and ~500 μm wide whereas for the same sliding distance under lubricated conditions, the wear track becomes very shallow (~0.75 μm deep and ~50 μm wide). For both cases in our experimental conditions, the substrate has not been exposed, as the depth of the wear track has been found smaller than the coating thickness of ~1.82 μm [15]. The wear coefficients for dry and lubricated sliding condition were found as 1.27 ×

10^{-15} $m^3N^{-1}m^{-1}$ and 9.62 × 10^{-17} $m^3N^{-1}m^{-1}$ respectively, which represents almost 13 times or 92.45% reduction compared to dry sliding.

3.2. Raman analysis

3.2.1. Raman analysis of as-deposited coated surface

The Raman spectrum of as-deposited C/Cr coated surface is shown in figure 4. The as-deposited coating is amorphous [15], therefore the spectrum only contains disordered and sp^2 bonded graphitic carbon peaks (D and G respectively). The average D and G positions are found to be 1383 cm^{-1} and 1575 cm^{-1} respectively. The average I_D/I_G ratio is calculated as 2.175.

3.2.2. Raman analysis of wear track after dry sliding

Figure 5 shows a Raman spectrum of the wear products in the wear track after 5 km of dry sliding. The spectrum contains typical graphitic carbon (D and G) peaks along with Cr_2O_3 and Cr_2N peaks and Fe_2O_3 and Fe_3O_4 peaks originating from the C/Cr coating and the counterpart respectively. The average D and G peak positions are found to be 1388 cm^{-1} and 1574 cm^{-1} respectively. The average I_D/I_G ratio is calculated as 2.254. The Cr_2N and Cr_2O_3 peaks appear at ~389 cm^{-1} and ~533 cm^{-1} respectively. A hump is seen in the spectrum at ~700 cm^{-1} and after deconvoluting the spectrum, a wide peak is found there centring at ~673 cm^{-1}. The peak has a width of ~280 cm^{-1} and therefore, it is believed that the peak is formed due to overlapping of three different peaks such as Cr_2O_3, Fe_2O_3 and Fe_3O_4. The Raman peaks of Cr_2O_3 is found at ~552 cm^{-1} and ~613 cm^{-1} (courtesy: ref [35] Table 5), whereas Fe_2O_3 and Fe_3O_4 have their corresponding Raman peaks at ~611− 613 cm^{-1} [36, 37] and ~661− 663 cm^{-1} [36, 37] respectively as already reported in literature.

Table 1 lists the Raman peaks found from wear track after dry sliding and then compares with the Raman peaks of those compounds already reported in literatures.

It is believed that Cr_2N originates from the CrN base layer due to occurrence of two simultaneous events such as, through slow nitrogen out diffusion and due to the reaction between the base layer of the coating and the nitrogen from atmosphere during sliding in air. The depth of wear track was found ~1.2 μm (from figure 3), which indicates that the CrN interlayer might be exposed during sliding against steel ball in air; however the substrate remained protected. Due to high flash temperature created at the asperity contacts during sliding, the CrN interlayer reacts with nitrogen from environment and forms Cr_2N. As the wear process continues, the nitrogen from the Cr_2N phase is depleted by the introduction of oxygen from the ambient atmosphere and metastable CrON phase is formed. The nitrogen from CrON is further replaced by oxygen and form very stable Cr_2O_3 [38]. The presence of Cr_2O_3 peaks indicate that the oxidation mechanism is based on the gradual replacement of nitrogen with oxygen during sliding. The Cr from the coating provides additional source for formation of Cr_2O_3 through direct reaction with oxygen. This reaction is promoted by the high flash temperatures generated at the asperity contacts during sliding.

As the depth of the wear track (~1.2 μm from figure 3) was found to be smaller than the thickness of the C/Cr coating (~1.82 μm) [15], it is therefore expected that the iron oxides (Fe_2O_3 and Fe_3O_4) cannot originate from the HSS substrate, but from the uncoated steel ball used as a counterpart. The compounds formed in the wear track in dry sliding as identified by the Raman studies lead to the conclusion that the wear mechanism in dry sliding can be described as mainly **oxidative reaction mechanism**. The equation set (1) lists the possible chemical reactions occurring during the dry sliding as follows:

$$4CrN + N_2 = 2Cr_2N + 2N_2$$
$$2Cr_2N + 3O_2 = 2Cr_2O_3 + N_2$$
$$4Fe + 3O_2 = 2Fe_2O_3$$
$$3Fe + 2O_2 = Fe_3O_4 \quad (1)$$

3.2.3. Raman analysis of wear track after lubricated sliding

Figure 6a shows the Raman spectrum of the thin oil film placed on a glass slide and figure 6b shows the spectrum of that dry glass slide. The oil peaks cannot be identified in figure 6a because the exact chemical compounds present in the oil are unknown. After lubricated sliding, the oil is carefully cleaned from the wear track, so that no trace of oil is left in the wear track but the wear products remain unaffected. Figure 7 shows the selected Raman spectrum indicating the wear products in the wear track after 5 km of lubricated sliding. The Raman spectrum of figure 6a and figure 7 does not match with each other, which indicates that the wear track is completely free from the oil when Raman spectrum is collected from the track after lubricated sliding.

The typical graphitic carbon (D and G) peaks appear in the Raman spectrum as shown in figure 7 along with peaks of different compounds such as Cr_2S_3, Cr_2N, CrN, Cr_2C, $CrCl_3$ and FeS_2. No oxide peaks are found, which was expected as the uncoated steel ball and the C/Cr coated disc were completely immersed into the engine oil during sliding and no direct contact with oxygen was possible unlike dry sliding. The average D and G peak positions are found to be 1383 cm^{-1} and 1573 cm^{-1} respectively. The average I_D/I_G ratio is calculated as 2.269. A clear $CrCl_3$ peak appears at ~204 cm^{-1}. Two wide peaks appear at two subsequent shoulders of the Raman spectrum centring at ~348 cm^{-1} and ~653 cm^{-1} respectively. These peaks have width of ~270 cm^{-1} and ~388 cm^{-1} respectively; therefore, it is believed that these peaks are formed due to overlapping of different compounds. The

peak centring at ~348 cm^{-1} and width of ~270 cm^{-1} is due to overlapping of Cr_2C, $CrCl_3$, Cr_2S_3, and FeS_2 peaks. The Raman peaks of Cr_2C, $CrCl_3$, and FeS_2 are found at ~344 cm^{-1} [39] and ~342±2 cm^{-1} [40] and ~341 cm^{-1} [41] respectively as already reported in literature. On the other hand, the peak centring at ~653 cm^{-1} and width of ~388 cm^{-1} is due to overlapping of Cr_2C, Cr_2N, CrN and Cr_2S_3 peaks. From the literature, the Raman peaks of Cr_2C are found at ~544 cm^{-1}, ~601 cm^{-1} and ~695 cm^{-1} [39] whereas Cr_2N and CrN have their respective Raman peaks at ~586 cm^{-1}, ~667 cm^{-1} and ~760 cm^{-1} [42] and ~660 cm^{-1} [42]. Due to unavailability of data on the Raman peaks of Cr_2S_3, a spectrum was collected from pure Cr_2S_3 powder as shown in figure 8. The peaks are found at ~301 cm^{-1}, ~341 cm^{-1}, ~536 cm^{-1} (most intense and sharp), ~602 cm^{-1} and ~1353 cm^{-1} respectively. Table 2 lists the Raman peaks obtained from the wear track after lubricated sliding and then compares with the Raman peaks of those compounds already reported in literatures.

Similar to the dry sliding case, the CrN base layer is converted to Cr_2N due to slow nitrogen out-diffusion, but could not be able to form stable Cr_2O_3 due to absence of oxygen during sliding. The presence of $CrCl_3$ and Cr_2S_3 peaks in the spectrum indicates a possible chemical reaction between coating and engine oil elements taking place during sliding. It has been reported that during sliding, abrasion occurs at the asperity contacts giving rise to flash temperature up to ~800°C. At that high temperature, the coating elements namely C and Cr react with sulphide and chloride compounds of the engine oil during sliding and form compounds such as $CrCl_3$ and Cr_2S_3 in the wear track. On the other hand, the FeS_2 peak indicates a similar tribochemical reaction between wear debris from the uncoated steel ball and the sulphide compounds from the oil. Therefore, the wear mechanism in lubricated sliding can be described as completely **tribo-chemically**

reactive. The equation set (2) lists the possible chemical reactions occurring during the lubricated sliding as follows:

$$\begin{aligned} C/Cr + sulphide - compounds\left(from \;\; oil \right) &\rightarrow Cr_2S_3 \\ C/Cr + chloride - compounds\left(from \;\; oil \right) &\rightarrow CrCl_3 \\ Fe + sulphide - compounds\left(from \;\; oil \right) &\rightarrow FeS_2 \end{aligned} \qquad (2)$$

4. Discussion

Figure 9 shows the comparison of Raman spectrum collected from as-deposited coating and wear track after both dry and lubricated sliding. During dry sliding, mainly oxidative reaction mechanism occurs within the wear track as already described in section 4.2.2. The oxidised wear debris is accumulated within the wear track during sliding. As a result, a hump is appeared at ~673 cm^{-1} of the spectrum unlike as-deposited surface. The hump indicates the presence of chromium oxide (Cr_2O_3) and iron oxides (Fe_2O_3 and Fe_3O_4) as reaction products during dry sliding.

Tribochemical reactions occur during lubricated sliding as previously explained in section 4.2.3. The as-deposited coating has chromium whereas the lubricant contains mostly sulphur and chlorine based compounds. As a result, Cr_2S_3 and $CrCl_3$ form during lubricated sliding via tribochemical reaction mechanism. The wear products accumulate within the wear track by forming a very thin layer. Figure 9 shows the overall increase of intensity of the spectrum due to formation of wear products when compared to the spectrum of as-deposited surface.

The I_D/I_G ratio is an important parameter in Raman analysis to estimate the disorder in the carbon network. The I_D indicates the intensity of D peak due to the A_{1g} breathing mode of carbon atoms in six fold rings. D peak is active only in presence of disorder and therefore this mode is absent in perfect graphite. On the other hand, the I_G indicates the intensity of graphitic (G) peak resulted from the E_{2g} stretching motion for all pairs of sp^2 bonded carbon atoms [28, 43 and 44]. The development of D peak, hence the increase in I_D/I_G ratio indicates disordering of graphite (according to Tuinstra–Koenig (TK) equation $\frac{I_D}{I_G} \propto \frac{1}{L_a}$) however ordering ($\frac{I_D}{I_G} \propto L_a^2$, TK equation is no longer valid) for amorphous carbon based films [28]. The nanostructured C/Cr coatings show clear and distinct D and G peaks in as-deposited condition (figure 4) as well as after both dry and lubricated sliding tests (figures 5 and 7). Therefore, an increase in I_D/I_G ratio indicates the rise in disordering for the C/Cr coatings.

Figure 10 shows that the I_D/I_G ratio increases after both dry and lubricated sliding when compared to the as-deposited condition. It can be speculated that the disorder increases due to the sliding action between coating and the counterpart. This in turn influences the friction behaviour. According to figure 10, the I_D/I_G ratio is found higher for lubricated sliding when compared to dry sliding. On the other hand, the coefficient of friction is found lower for lubricated sliding when compared to dry sliding as shown in figure 2. Therefore, I_D/I_G ratio varies inversely with the coefficient of friction and wear. The continuous rubbing of 100Cr6 steel ball against the wear debris during 5 km of sliding causes severe plastic deformation of the debris, which ultimately results in reduction of cluster size. The lower cluster size increases the breathing mode of six fold rings leading to the development of D peak and therefore an increase in D peak intensity is observed. However, it does not affect the stretching motion of sp^2 bonded carbon atoms leading to the no change in the G peak intensity. As a result, the I_D/I_G ratio is increased indicating

the rise in disordering of the carbon network. This is supported by the fact that the I_D/I_G ratio increases for nanocrystalline graphite, when the cluster size decreases (courtesy: ref [28], figure 5). Therefore, it is believed that increase in disorder in carbon network helps to reduce the coefficient of friction due to the irregularity of bonds which in turn weakens the material.

Figure 11 shows the individual intensities of D and G bands for as-deposited coating and both the dry and lubricated sliding cases. The I_D and I_G both are found lowest when spectrum is collected from as-deposited surface. In case of both dry and lubricated sliding, the I_D and I_G individually increases compared to as-deposited surface. The I_D and I_G both are found highest for lubricated sliding condition. The D peak height is found higher in lubricated sliding (~107.5) when compared to dry sliding (~93), however the G peak height is found almost similar (~41−47) irrespective of sliding conditions. The rise in I_D in lubricated sliding indicates the increase in disordering compared to dry sliding case and explains the reason of higher I_D/I_G ratio found for lubricated sliding.

4.1. The tribo-chemical wear mechanism

In boundary lubricated condition, the temperature at the asperity contacts increases due to continuous rubbing between C/Cr coated disc and uncoated steel ball and it could reach up to ~800°C. The chlorine and sulphur containing compounds of the engine oil become reactive in that high temperature and chemically react with the C/Cr coating and the uncoated steel ball at the asperity contacts. The reaction products are mostly chromium sulphide (Cr_2S_3) and chromium chloride ($CrCl_3$) as already established by Raman analysis. These compounds adhere to the wear track forming a thin tribolayer.

The lubricated friction behaviour in figure 2 indicates a very short initial run-in period and then a steady state sliding up to 5 km of sliding distance. This behaviour is dedicated to the formation of the thin tribolayer containing Cr_2S_3 and $CrCl_3$. Figure 12 shows the atomic structure of $CrCl_3$, in which Cr^{+3} cations occupy two-third of the octahedral structure and the Cl^- anions form a cubic closed packed structure around it resulting in a layered arrangement. Figure 13 illustrates one such octahedral structure having Cr^{+3} cation at the centre and Cl^- anions placed at the edges. The octahedral structures are bonded with each other by sharing the edges and form stacking of $CrCl_3$ layers. Therefore, two adjacent atomic layers of $CrCl_3$ are bonded due to sharing of Cl^- anions, which makes the bonding weak due to the absence of cohesive effect of Cr^{+3} cations. The weak bonding between adjacent atomic layers helps the $CrCl_3$ atomic planes to easily slide over another indicating its lubricant nature [45]. Figure 14 shows the stacking of layers in the $CrCl_3$ crystal structure that promotes slipping during sliding. It is believed that this lubricious compound $CrCl_3$ is responsible for further reducing the friction coefficient during lubricated sliding and increased coating-life due to higher wear resistance. Moreover, it has been found that the Cr_2S_3 has hexagonal crystal structure unlike $CrCl_3$. The hexagonal structure does not promote any slipping between atomic planes therefore Cr_2S_3 does not help in reducing friction.

Hence, it could be concluded that, C/Cr coating helps in reducing friction coefficient in boundary lubrication condition due to the formation of solid lubricants such as $CrCl_3$ via tribo-chemical reaction mechanism.

5. Conclusion

A C/Cr coating has been deposited on hardened (62 HRC) high speed steel substrate by a combined steered cathodic arc and unbalanced magnetron process known as Arc-Bond-Sputtering (ABS) technique. Sliding tests have been performed in dry and lubricated condition in order to investigate the wear products generated during siding and to understand the wear mechanism.

The average friction coefficients of C/Cr coating during dry and lubricated sliding conditions have been found to be 0.22 and 0.12 respectively, indicating a significant reduction (~45.5%) during lubricated sliding. Similarly, the wear coefficient has been reduced from 1.27×10^{-15} $m^3N^{-1}m^{-1}$ to 9.62×10^{-17} $m^3N^{-1}m^{-1}$ due to the addition of lubricant.

The wear mechanism of C/Cr coating has been investigated by Raman spectroscopy. The wear mechanism during dry sliding has been found mainly oxidative whereas during boundary lubricated sliding, it is chemically reactive. The I_D/I_G ratio is increased for both dry and lubricating sliding conditions when compared to as-deposited surface. The Raman spectrum taken from the wear track after lubricated sliding indicates the formation of lubricious compound $CrCl_3$, which has graphite-like layer-by-layer structure. Therefore, it has been considered as the key factor for reducing the friction coefficient significantly during lubricated sliding.

References:

[1] Zeng X.T., Zhang S., Ding X.Z., Teer D.G. Comparison of three types of carbon composite coatings with exceptional load-bearing capacity and high wear resistance. Thin Solid Films. 2002; 420 –421: 366–370

[2] Yang S., Camino D., Jones A.H.S., Teer D.G. Deposition and tribological behaviour of sputtered carbon hard coatings. Surface and Coatings Technology 2000; 124: 110–116

[3] Erdemir A., Donnet C. Tribology of diamond-like carbon films: recent progress and future prospects. J. Phys. D: Appl. Phys. 2006; 38: R301–R316

[4] Grill A. Diamond-like carbon: state of the art. Diamond and Related Materials. 1999; 8: 428–434

[5] Zaidi H., Le Huu T., Paulmier D. Influence of hydrogen contained in hard carbon coatings on their tribological behaviour. Diamond and Related Materials. 1994; 3: 787-790

[6] Walter K.C., Kung H., Levine T., Tesmer J.T., Kodali P., Wood B.P., Rej D.J., Nastasi M., Koskinen J., Hirvonen J.P. Characterization and performance of diamond-like carbon films synthesized by plasma- and ion-beam-based techniques. Surface and Coatings Technology. 1995; 74-75: 734-738

[7] Ma G., Gong S., Lin G., Zhang L., Sun G. A study of structure and properties of Ti-doped DLC film by reactive magnetron sputtering with ion implantation. Applied Surface Science. 2012: 258: 2945– 2950

[8] Wu W. J., Hon M. H., Thermal stability of diamond-like carbon films with added silicon. Surface and Coatings Technology. 1999; 111: 133–140

[9] Yang S., Teer D.G., Investigation of sputtered carbon and carbonrchromium multi-layered coatings. Surface and Coatings Technology. 2000; 130: 412-416

[10] Yang S., Li X., Renevier N.M., Teer D.G. Tribological properties and wear mechanism of sputtered C/Cr coating. Surface and Coatings Technology. 2001; 142−144 : 85−93

[11] Ban M., Hasegawa T. Internal stress reduction by incorporation of silicon in diamond-like carbon films. Surface and Coatings Technology. 2002; 162 :1–5

[12] Corbella C., Oncins G., Gomez M.A., Polo M.C., Pascual E., Garcia-Cespedes J., Andujar J.L., Bertran E., Structure of diamond-like carbon films containing transition metals deposited by reactive magnetron sputtering. Diamond & Related Materials. 2005; 14: 1103–1107

[13] Baba K., Hatada R., Preparation and properties of metal-containing diamond-like carbon films by magnetron plasma source ion implantation. Surface & Coatings Technology. 2005; 196: 207– 210

[14] Kok Y.N., Hovsepian P.Eh., Resistance of nanoscale multilayer C/Cr coatings against environmental attack. Surface & Coatings Technology. 2006; 201: 3596–3605

[15] Kok Y.N., Hovsepian P.Eh., Luo Q., Lewis D.B., Wen J.G., Petrov I. Influence of the bias voltage on the structure and the tribological performance of nanoscale multilayer C/Cr PVD coatings. Thin Solid Films. 2005; 475: 219– 226

[16] Pal S. K., Jiang J., Meletis E.I. Effects of N-doping on the microstructure, mechanical and tribological behavior of Cr-DLC films. Surface & Coatings Technology. 2007; 201: 7917–7923
[17] Dai W., Wang A. Synthesis, characterization and properties of the DLC films with low Cr concentration doping by a hybrid linear ion beam system. Surface and Coatings Technology. 2011; 205: 2882-2886
[18] Singh V., Jiang J.C., Meletis E.I. Cr-diamond like carbon nanocomposite films: Synthesis, characterization and properties. Thin Solid Films. 2005; 489: 150 – 158
[19] Dai W., Ke P., Wang A. Microstructure and property evolution of Cr-DLC films with different Cr content deposited by a hybrid beam technique. Vacuum. 2011; 85: 792-797
[20] Sun J., Fu Z., Zhang W., Wang C., Yue W., Lin S., Dai M., Friction and wear of Cr-doped DLC films under different lubrication conditions. Vacuum. 2013; 94: 1-5
[21] Hovsepian P.Eh., Kok Y.N., Ehiasarian A.P., Erdemir A., Wen J.G., Petrov I., Structure and tribological behaviour of nanoscale multilayer C / Cr coatings deposited by the combined steered cathodic arc/unbalanced magnetron sputtering technique. Thin Solid Films. 2004; 447 – 448: 7–13
[22] Czyzniewski A. Mechanical and Tribological Properties of Cr-DLC Coatings Deposited by ARC-MAG-RF PACVD Hybrid Method. Plasma Process. Polym. 2007; 4: S225–S230
[23] Ronkainen H., Varjus S., Holmberg K. Tribological performance of different DLC coatings in water-lubricated conditions. Wear. 2001; 249: 267–271
[24] Münz, W.D., Schulze, D., and Hauzer, F.J.M. A new method for hard coatings: ABS TM (arc bond sputtering). Surface and Coatings Technology. 1992, 50: 169-178
[25] Hovsepian P.Eh., Kok Y.N., Ehiasarian A.P., Haasch R., Wen J.-G., Petrov I. Phase separation and formation of the self-organised nanostructure in C/Cr coatings in conditions of high ion irradiation. Surface & Coatings Technology. 2005; 200:1572-1579
[26] http://www.mobil.co.uk/UK-English-LCW/carengineoils_products_mobil-1-extended-life-10w60.aspx#
[27] Standard Test Method for Sulfated Ash from Lubricating Oils and Additives, Designation: D 874 – 00
[28] Ferrari A. C. and Robertson J. Interpretation of Raman spectra of disordered and amorphous carbon. Phisycal review B. 2000; 61; 20
[29] Ogwu A.A., Lamberton R.W., Morley S., Maguire P., McLaughlin J. Characterisation of thermally annealed diamond like carbon (DLC) and silicon modified DLC films by Raman spectroscopy. Physica B. 1999; 269: 335-344
[30] Leu Ming-Sheng, Chen S.Y., Chang J.J., Chao L.G., Lin W. Diamond-like coatings prepared by the filtered cathodic arc technique for minting application. Surface and Coatings Technology. 2004; 177 –178: 566–572
[31] Cui W.G., Lai Q.B., Zhang L., Wang F.M. Quantitative measurements of sp3 content in DLC films with Raman spectroscopy. Surface & Coatings Technology. 2010; 205: 1995–1999

[32] Zhao J. F., Lemoine P., Liu Z. H., Quinn J. P., McLaughlin J. A.. The effects of Si incorporation on the microstructure and nanomechanical properties of DLC thin films. J. Phys.: Condens. Matter. 2000; 12: 9201–9213.

[33] Sheeja D., Tay B.K., Lau S.P., Shi X., Ding X. Structural and tribological characterization of multilayer ta-C films prepared by filtered cathodic vacuum arc with substrate pulse biasing. Surface and Coatings Technology. 2000; 132: 228-232

[34] Tai F. C., Lee S. C., Chen J., Wei C., Chang S. H. Multi peak fitting analysis of Raman spectra on DLCH film. Journal of Raman Spectroscopy. 2009; 40: 1055–1059

[35] Maslar J.E., Hurst W.S., Bowers W.J. Jr., Hendricks J.H., Aquino M.I., Levin I. In situ Raman spectroscopic investigation of chromium surfaces under hydrothermal condition. Applied Surface Science. 2001; 180: 102-118

[36] Wei Q., Li Z., Zhang Z., Zhou Q. Facile Synthesis of α-Fe_2O_3 Nanostructured Films with Controlled Morphology. Materials Transactions. 2009; Vol. 50, No. 6 pp. 1351 to 1354

[37] Faria D. L. A., Silva S. V., Oliveira M. T.**,** Raman Microspectroscopy of Some Iron Oxides and Oxyhydroxides. Journal of Raman Spectroscopy. 1997; vol. 28, 873-878

[38] Zhou Z., Ross I. M., Ma L., Rainforth W. M., Ehiasarian A. P., Hovsepian P., Wear of hydrogen free C/Cr PVD coating against Al_2O_3 at room temperature. Wear. 2011; 271: pp. 2150-2156

[39] Zhu Y., Wang L., Yao W., Cao L., The interface diffusion and reaction between Cr layer and diamond particle during metallization. Applied Surface Science. 2001; 171: 143-150

[40] Sowden R.E., Orza J.M., Nontero S., Vibrational spectra of anhydrous chromium(III) chloride. Polyhedron. 1982; Vol.I, No.5. pp. 475-477

[41] Boughriet A., Ouddane B., Cordier C. and Laureyns J. Thermodynamic, spectroscopic and magnetic studies on anoxic sediments from the Seine river estuary**,** J. Chem. Soc., Faraday Trans. 1998; 94: 3677-3683

[42] Barata A., Cunha L., Moura C., Characterisation of chromium nitride films produced by PVD techniques. Thin Solid Films, 2001; 398 –399: 501–506

[43] Tuinstra F. and Koenig J. L. Raman Spectrum of Graphite. The Journal of Chemical Physics. 1970 August; volume 53, number 3

[44] Irmer G., Dorner-Reisel A. Micro-Raman studies on DLC coating. Advanced Engineering Materials. 2005; 7: No. 8

[45] Greenwood N. N., Earnshaw A. Chemistry of the Elements, Butterworth-Heinemann, 2nd edition, 1997, Chapter 23, p. 1020

[46] http://en.wikipedia.org/wiki/File:Chromium(III)-chloride-sheet-from-monoclinic-xtal-3D-balls.png

[47] http://en.wikipedia.org/wiki/File:Chromium(III)-chloride-monoclinic-xtal-Cr-coordination-3D-balls.png

[48] http://en.wikipedia.org/wiki/File:Chromium(III)-chloride-layers-stacking-from-monoclinic-xtal-3D-balls.png

Table 1: Comparison of Raman peaks of compounds found from wear track after dry sliding and the Raman peaks of same compounds found from literature

Raman peaks assigned to	Raman peaks (this work)	Raman peaks (literature)
Cr_2N	~ 389 cm^{-1}	~ 385 cm^{-1} [42]
Cr_2O_3	~ 533 cm^{-1}	~ 527 − 530 cm^{-1} [35]
Cr_2O_3	~ 673 cm^{-1} with a width of ~ 280 cm^{-1}	~552 cm^{-1} and ~613 cm^{-1} [35]
Fe_2O_3		~611− 613 cm^{-1} [36, 37]
Fe_3O_4		~661− 663 cm^{-1} [36, 37]

Table 2: Comparison of Raman peaks found from wear track after lubricated sliding and the Raman peaks of same compounds found from literature

Raman peaks assigned to	Raman peaks (this work)	Raman peaks (literature)
$CrCl_3$	~ 204 cm^{-1}	~ 207.5±2 cm^{-1} [40]
Cr_2C	~ 348 cm^{-1} with a width of ~ 270 cm^{-1}	~344 cm^{-1} [39]
$CrCl_3$		~342±2 cm^{-1} [40]
Cr_2S_3		—
FeS_2		~341 cm^{-1} [41]
Cr_2C	~653 cm^{-1} with a width of ~388 cm^{-1}	~544 cm^{-1}, ~601 cm^{-1} and ~695 cm^{-1} [39]
Cr_2N		~586 cm^{-1}, ~667 cm^{-1} and ~760 cm^{-1} [42]
CrN		~660 cm^{-1} [42]
Cr_2S_3	~536 cm^{-1}	—

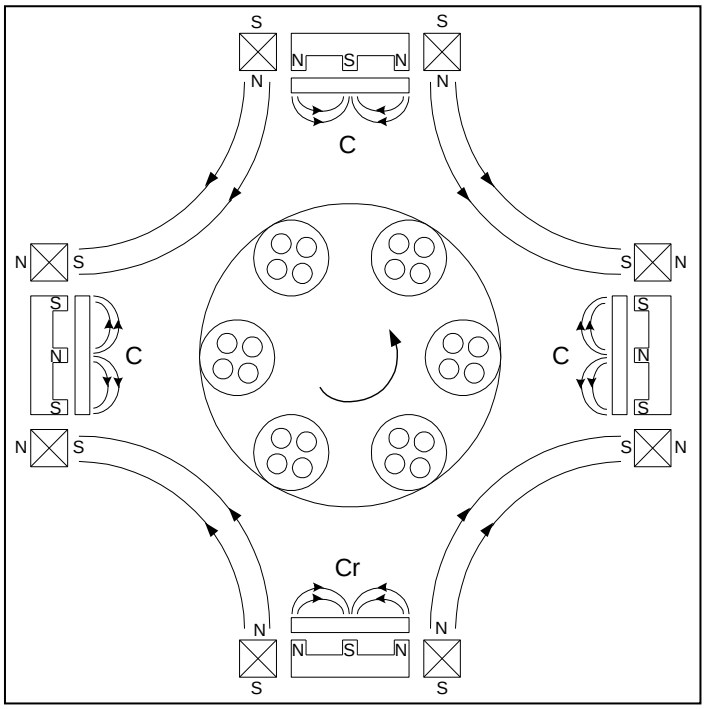

Figure 1: Schematic diagram of the cathode configuration in HTC 1000-4 PVD coating machine

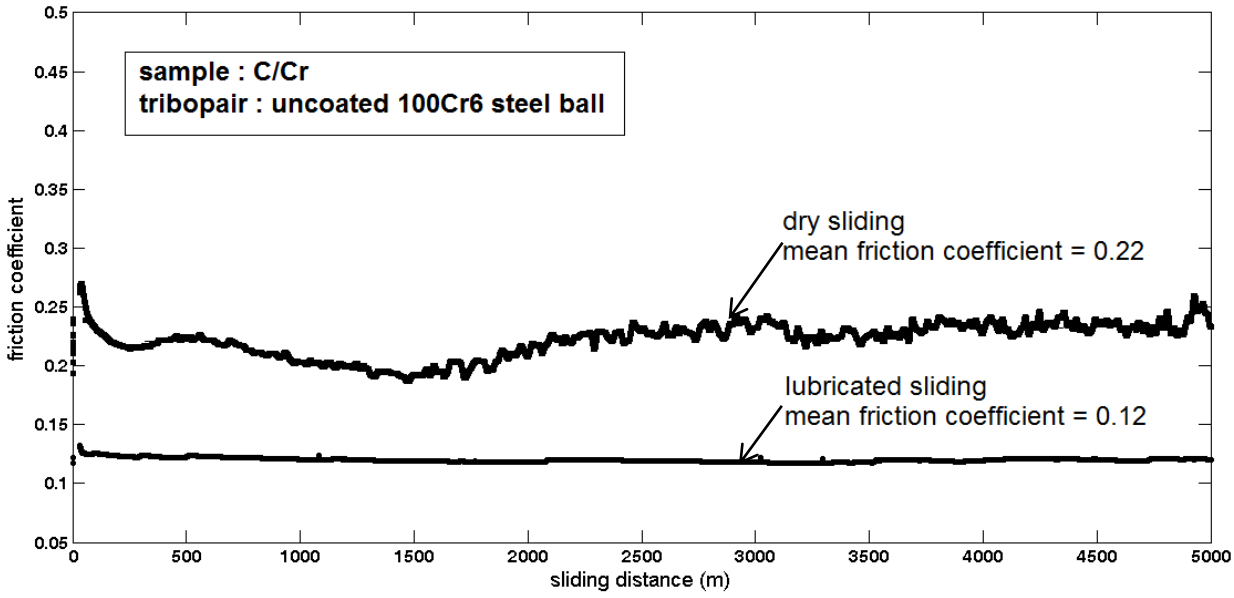

Figure 2: Friction behaviour of C/Cr coating against uncoated 100Cr6 steel ball under both dry and lubricated sliding

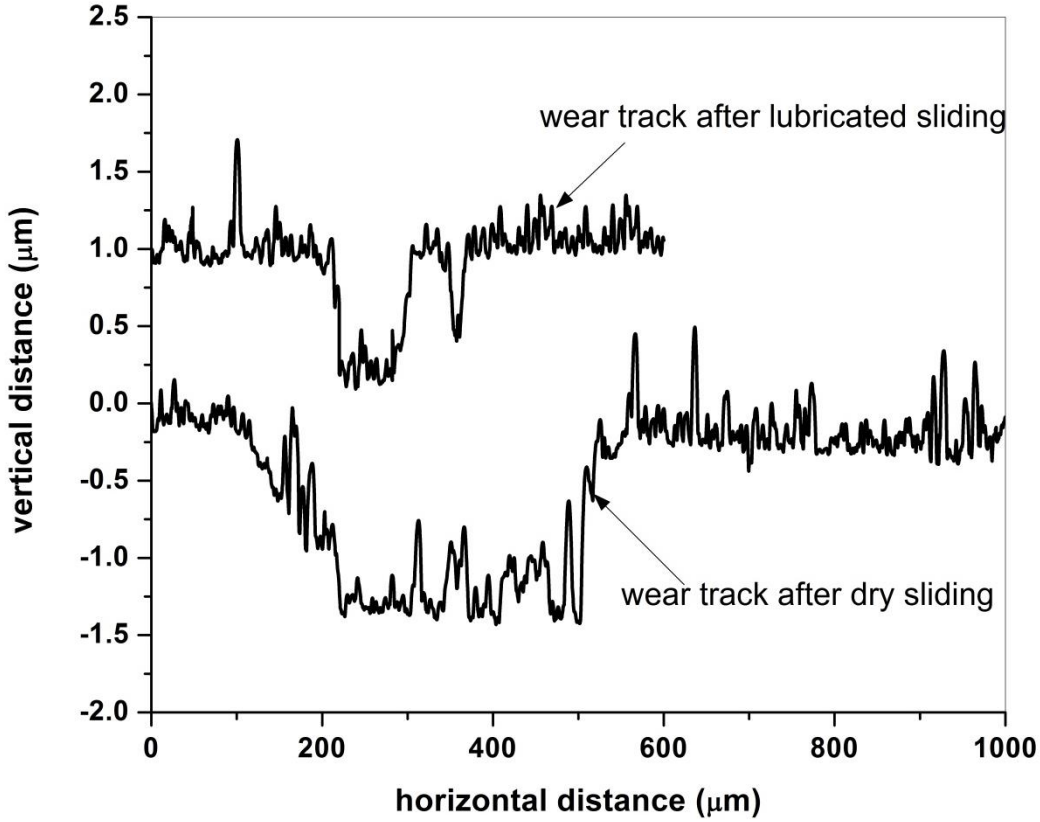

Figure 3: Wear track profiles of C/Cr coating after both dry and lubricated sliding

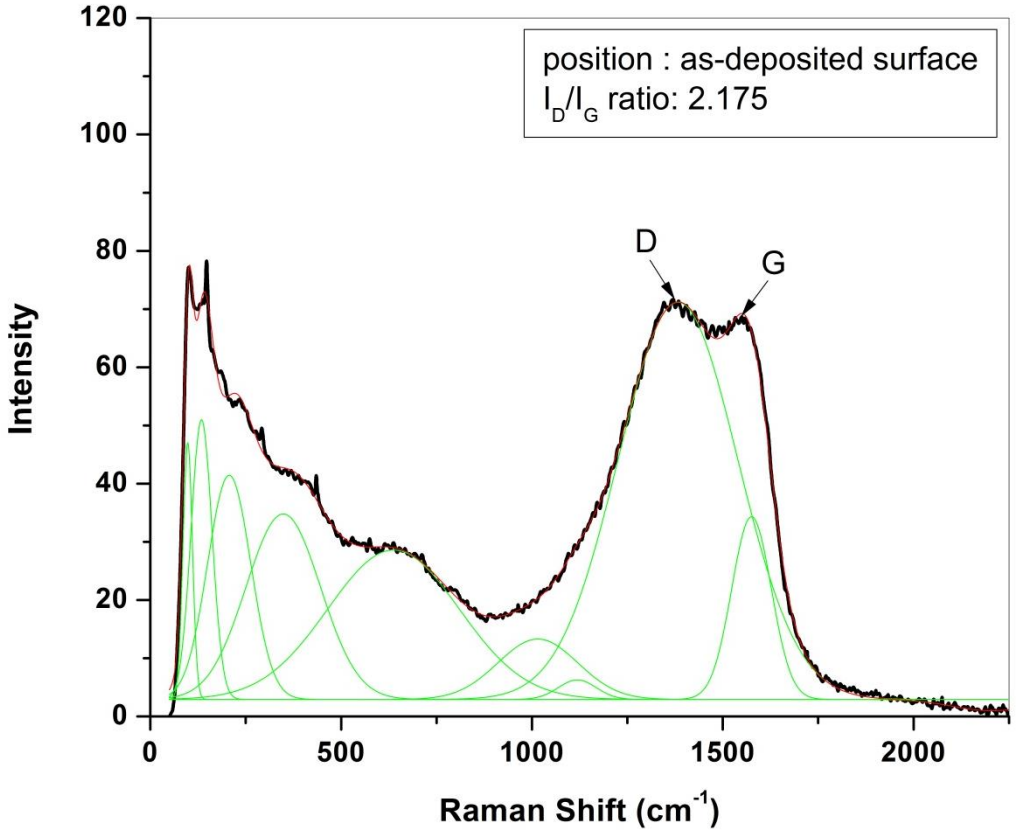

Figure 4: Raman spectrum of as-deposited C/Cr coating

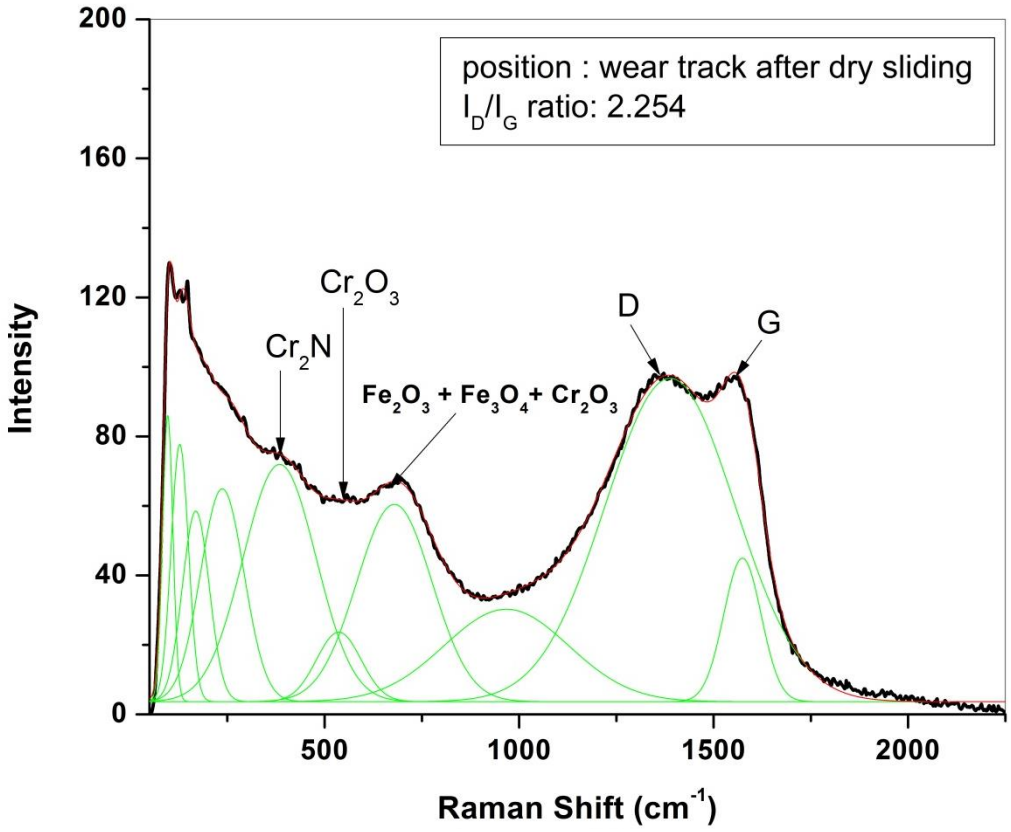

Figure 5: Raman spectrum showing the presence of different phases within the wear track after dry sliding

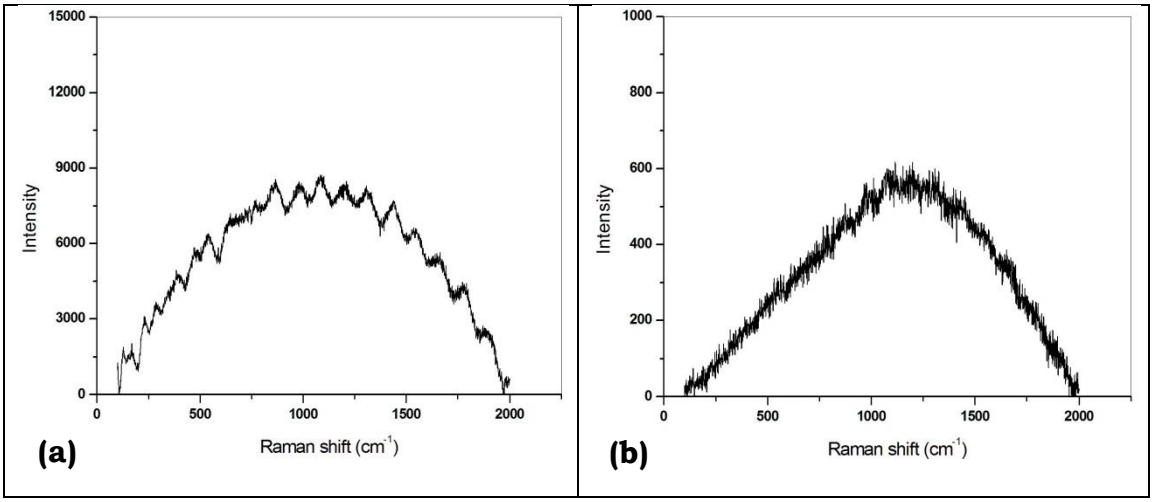

Figure 6: (a) Raman spectrum of thin oil film placed on a glass slide and (b) Raman spectrum of the glass slide.

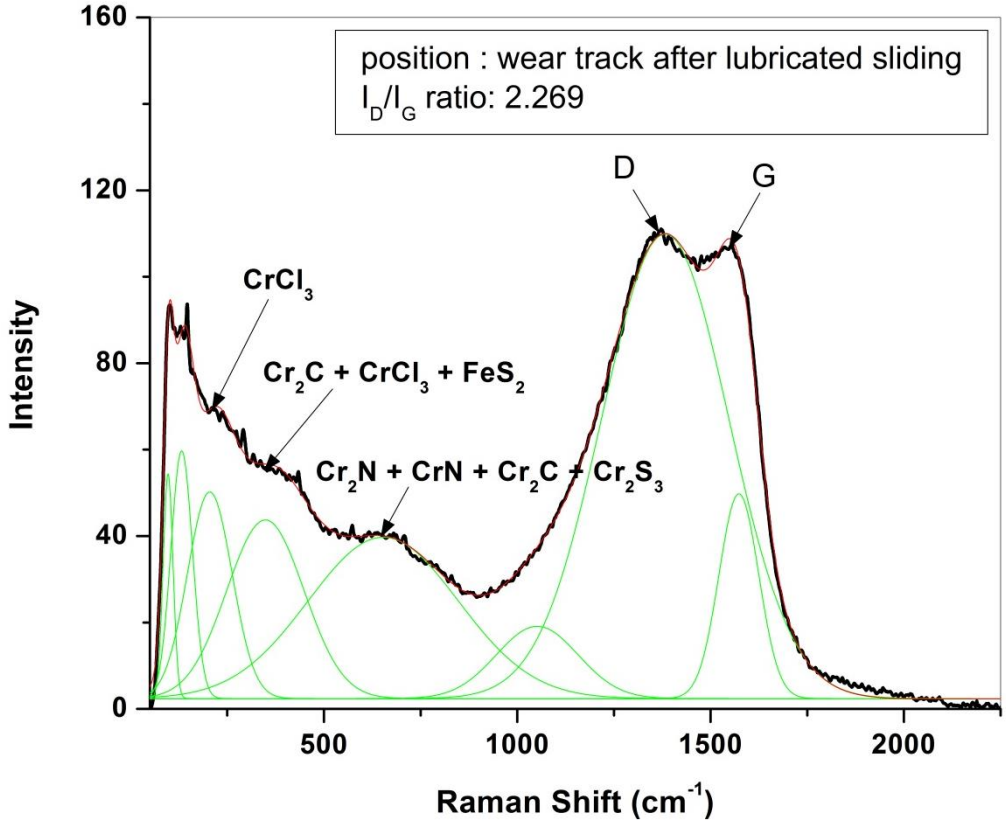

Figure 7: Raman spectrum showing the presence of different phases within the wear track after lubricated sliding

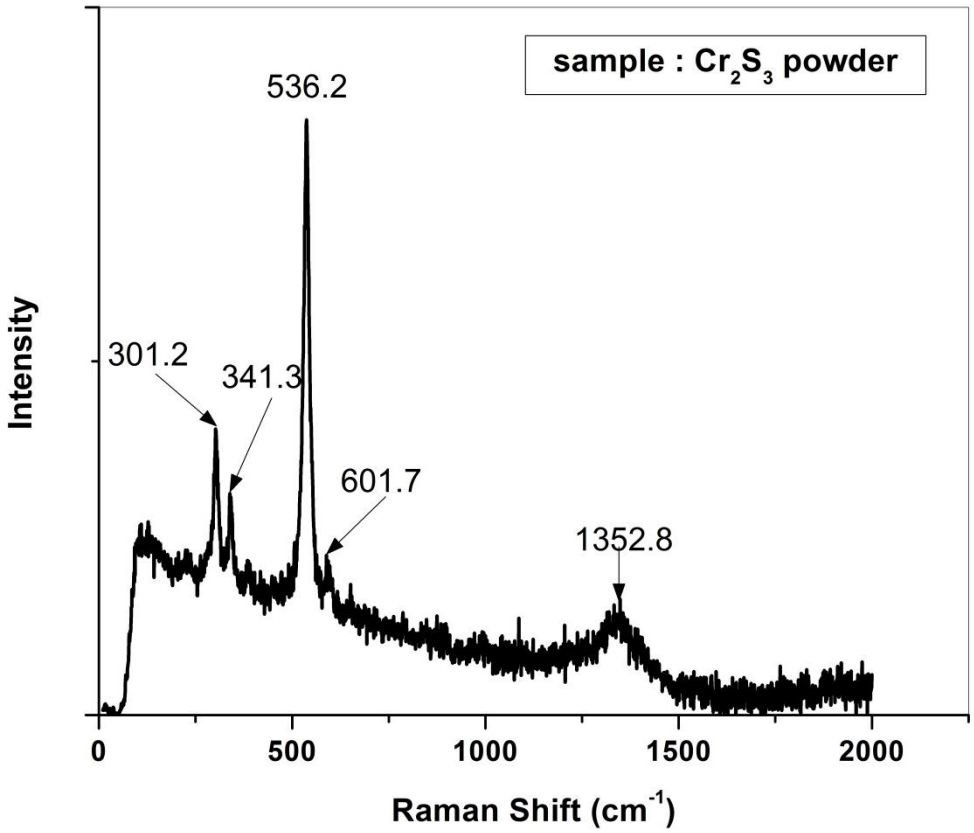

Figure 8: Raman spectrum of Cr_2S_3 powder sample

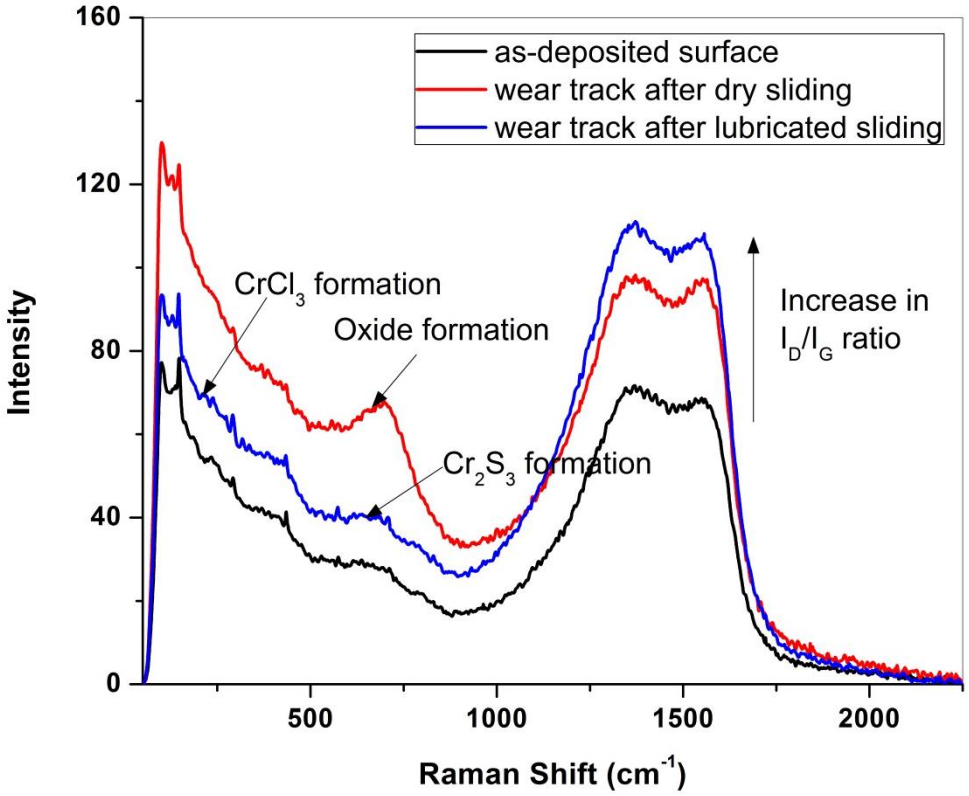

Figure 9: Comparison of Raman spectra collected from as-deposited coating and from the wear track after both dry and lubricated sliding

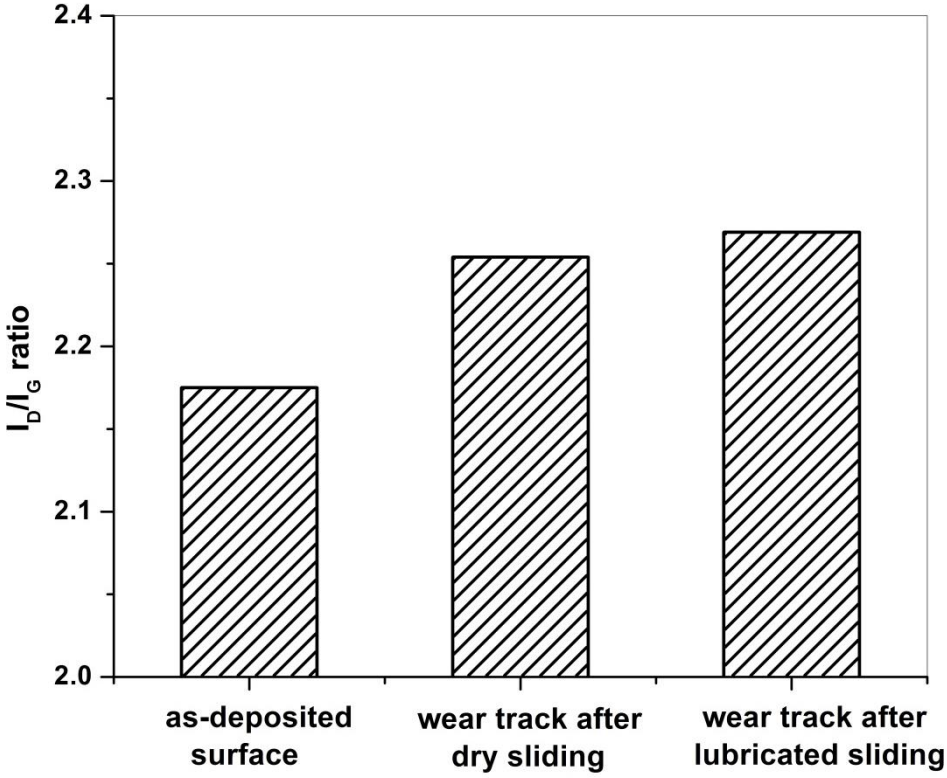

Figure 10: Comparison of I_D/I_G ratio of the as-deposited coating and the wear track after both dry and lubricated sliding

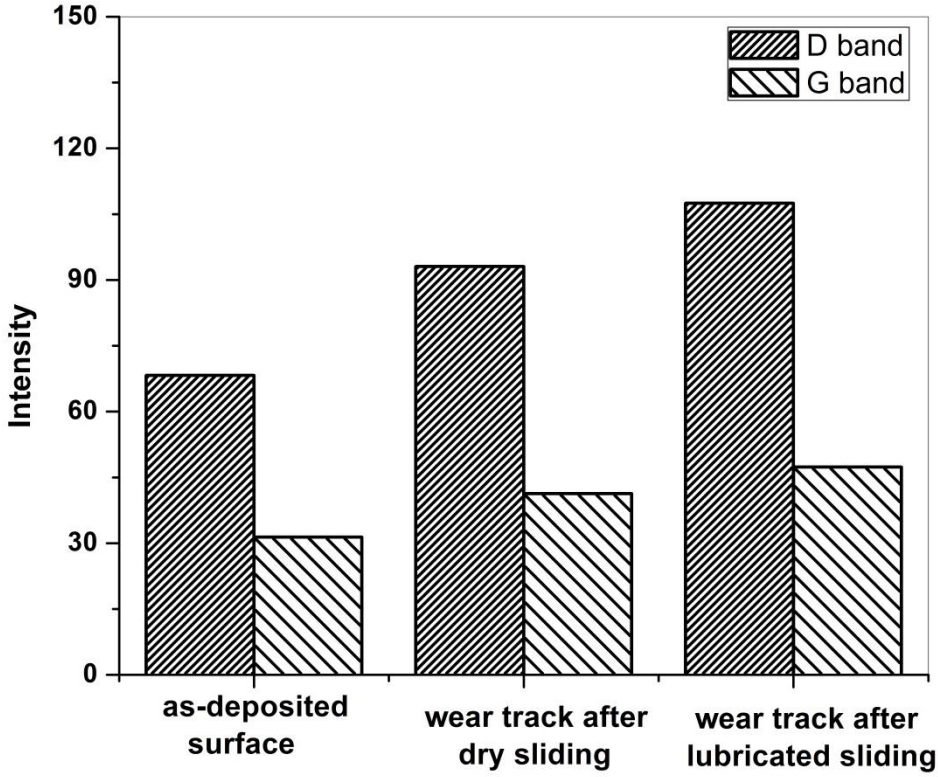

Figure 11: Comparison of D and G band intensities of the as-deposited coating and the wear track after both dry and lubricated sliding

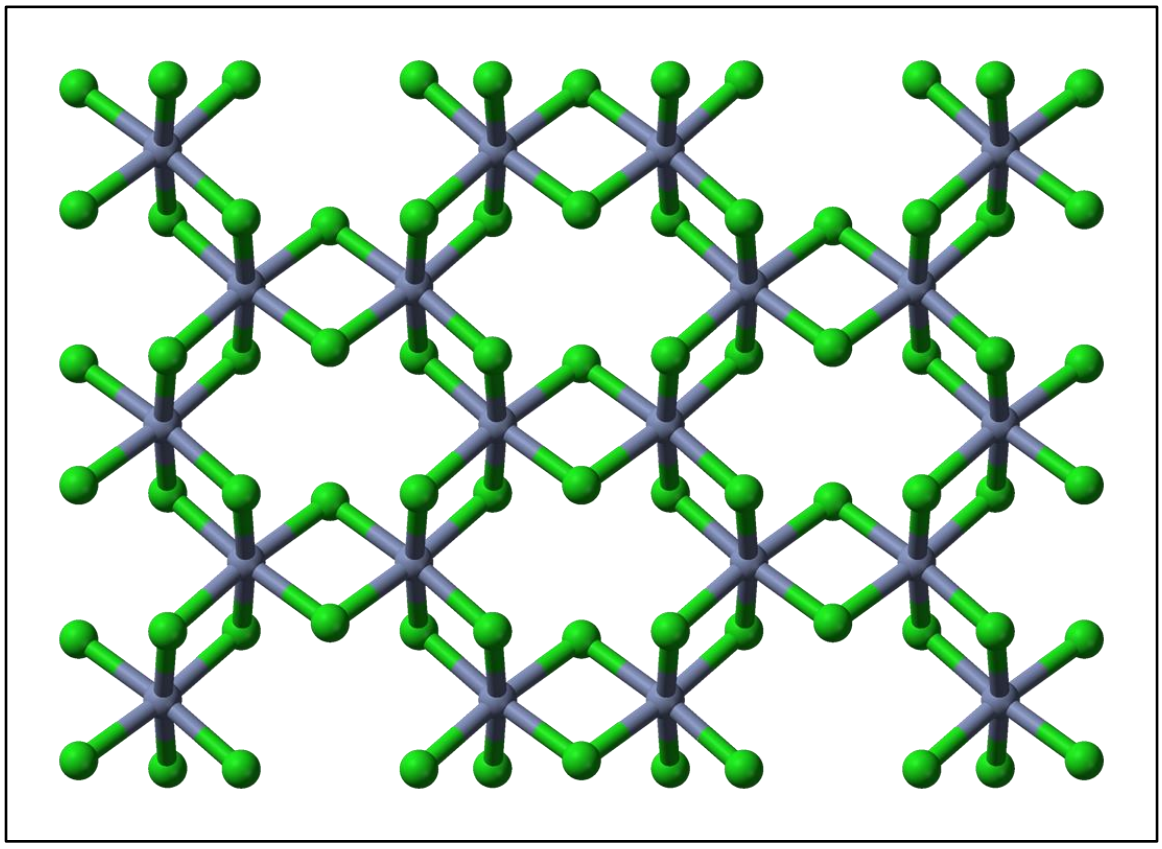

Figure 12: Atomic structure of $CrCl_3$ [46]

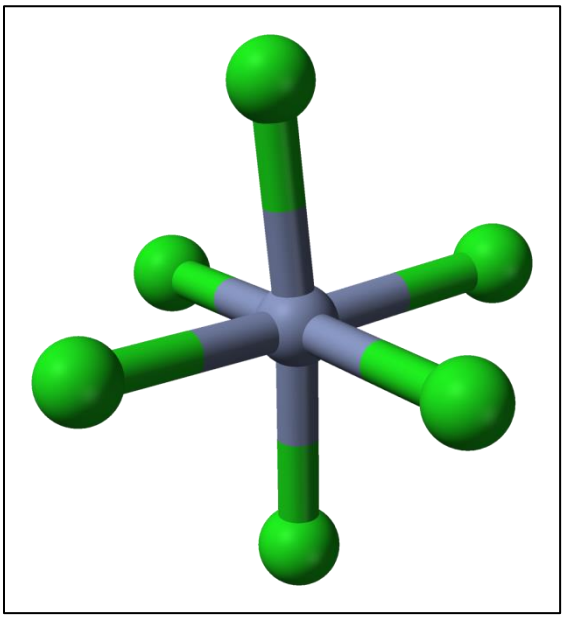

Figure 13: Octahedral structure of $CrCl_3$ molecule having Cr^{+3} cation at the centre and Cl^- anions at the edges [47]

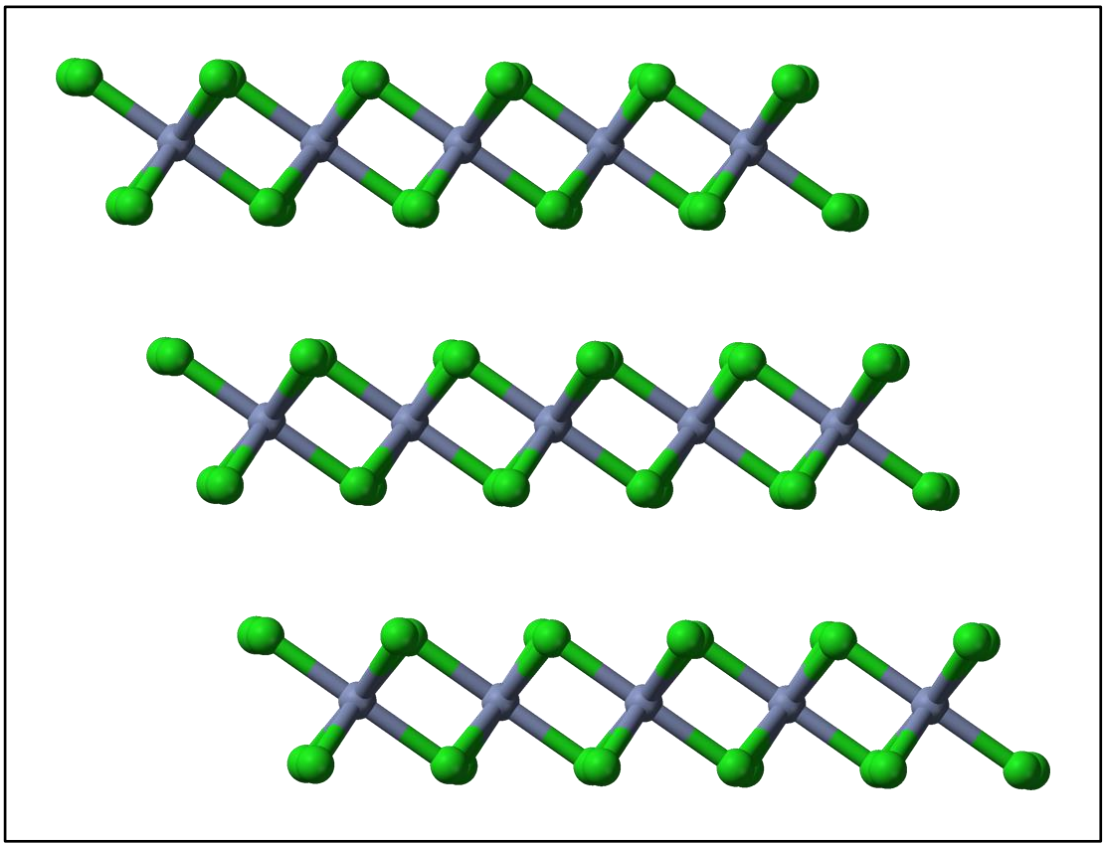

Figure 14: The stacking of layers in $CrCl_3$ crystal structure [48]